Analysis of the Subcellular Phosphoproteome Using a Novel Phosphoproteomic Reactor

ARTICLE *in* JOURNAL OF PROTEOME RESEARCH · MARCH 2010

Impact Factor: 4.25 · DOI: 10.1021/pr900767j · Source: PubMed

9 AUTHORS, INCLUDING:

Houjiang Zhou
University of Ottawa
44 PUBLICATIONS **1,586** CITATIONS
SEE PROFILE

Ruijun Tian
Samuel Lunenfeld Research Institute
34 PUBLICATIONS **1,192** CITATIONS
SEE PROFILE

Hu Zhou
Shanghai Jiao Tong University
156 PUBLICATIONS **2,397** CITATIONS
SEE PROFILE

Daniel Figeys
University of Ottawa
190 PUBLICATIONS **8,766** CITATIONS
SEE PROFILE

research articles Journal of proteome research

Analysis of the Subcellular Phosphoproteome Using a Novel Phosphoproteomic Reactor

Houjiang Zhou,[†,‡,||] Fred Elisma,[†,‡] Nicholas J. Denis,[†,‡] Theodore G. Wright,[†,‡] Ruijun Tian,[†,‡] Hu Zhou,[†,‡] Weimin Hou,[†,§] Hanfa Zou,[*,||] and Daniel Figeys[*,†,‡,§]

Ottawa Institute of Systems Biology, Department of Biochemistry, Microbiology and Immunology, Faculty of Medicine, and Department of Chemistry, University of Ottawa, 451 Smyth Road, Ottawa, Ontario, Canada K1H 8M5, and Key Laboratory of Separation Science for Analytical Chemistry and National Chromatographic R&A Center, Dalian Institute of Chemical Physics, Chinese Academy of Sciences, 457 Zhongshan Road, Dalian, China 116023

Received August 28, 2009

Protein phosphorylation is an important post-translational modification involved in the regulation of many cellular processes. Mass spectrometry has been successfully used to identify protein phosphorylation in specific pathways and for global phosphoproteomic analysis. However, phosphoproteomics approaches do not evaluate the subcellular localization of the phosphorylated forms of proteins, which is an important factor for understanding the roles of protein phosphorylation on a global scale. The in-depth mapping of protein phosphorylation at the subcellular level necessitates the development of new methods capable of specifically and efficiently enriching phosphopeptides from highly complex samples. Here, we report a novel microfluidic device called the phosphoproteomic reactor that combines efficient processing of proteins followed by phosphopeptide enrichment by Ti-IMAC. To illustrate the potential of this novel technology, we mapped the phosphoproteins in subcellular organelles of liver cells. Fifteen subcellular fractions from liver cell cultures were processed on the phosphoproteomic reactor in combination with nano-LC-MS/MS analysis. We identified thousands of phosphorylation sites in over 600 phosphoproteins in different organelles using minute amounts of starting material. Overall, this approach provides a new avenue for studying the phosphoproteome of the subcellular organelles.

Keywords: Phosphoproteomics • proteomic reactor • subcellular • technology

Introduction

Reversible protein phosphorylation is the most common post-translation modification (PTM) that is involved in a variety of fundamental cellular functions in living cells such as receptor-mediated signal transduction, cell cycle control, proliferation, differentiation, and apoptosis.[1,2] Deregulated phosphorylation signaling is a hallmark of cancer and other diseases, and protein kinases and phosphatases are prominent drug targets.[2,3] The understanding of the function of protein phosphorylations in regulating biological processes is limited by technology to identify protein phosphorylations and their subcellular localization. This is often compounded by the abundance, high dynamic range, low stoichiometry and heterogeneity of protein phosphorylations.[4,5]

Novel technologies for specifically enriching phosphoproteins and phosphopeptides have been developed, in particular, technologies that are based on antibody,[1,6] and ionic and chemical interactions.[7,8] The most common strategies to enrich phosphopeptides are based on IMAC with chelated Fe^{3+} or Ga^{3+},[7,8] and on metal oxide chromatography such as titanium dioxide[9] and zirconium dioxide.[10] Unfortunately, one of the major limitations associated with these strategies is the adsorption of acidic peptides which competes with the purification of phosphorylated peptides and reduces the sensitivity and specificity of the technologies.[11] The adsorption of acidic peptides can be reduced by *O*-methyl esterification with IMAC, or competitive binders (2,5-dihydroxybenzoic acid, phthalic acid, lactic acid and β-hydroxypropanoic acid) in combination with metal oxides.[9,12−15] More recently, SIMAC,[16] HILIC[17] and a new IMAC chelated with titanium or zirconium by phosphate group ligands[18,19] were also shown to be promising enrichment techniques. A comparison of different phosphopeptide enrichment methods that includes phosphoramidate chemistry,[20] IMAC, and TiO_2 chromatography has shown that each method isolated different and partially overlapping segments of a phosphoproteome which indicates that no single method can map a whole phosphoproteome.[21]

The complexity of the proteome is a challenge for many bioanalytical techniques, and various approaches have been developed to reduce the complexity of the proteome.[22−24] In particular, subcellular fractionation of organelles reduces the

* To whom correspondence should be addressed. E-mail: (D.F.)dfigeys@uottawa.ca; (H.Z.) hanfazou@dicp.ac.cn.
† Ottawa Institute of Systems Biology, University of Ottawa.
‡ Department of Biochemistry, Microbiology and Immunology, Faculty of Medicine, University of Ottawa.
|| Dalian Institute of Chemical Physics, Chinese Academy of Sciences.
§ Department of Chemistry, University of Ottawa.

10.1021/pr900767j

Published on Web 01/12/2010

complexity of the proteome while providing information on the localization of the proteins.[25−27] For example, subcellular fractionation was used to study 1404 proteins from a mouse liver.[27] Emili and co-workers separated the cell lysate from six different mouse tissues into cytosolic, nuclear, mitochondrial and membrane fractions and obtained subcellular information on more than 5000 proteins.[26] Gilchrist et al. reported the quantitative analysis of more than 1400 proteins in the secretory pathway using spectral counting.[25] Furthermore, isotope tagging was also used for the quantitative analysis of organelle proteomes.[28] This strategy was used to study the *Arabidopsis* organelle proteomes,[29] rat liver mitochondria proteomes,[30] and DT40 lymphocyte cell organelle proteomes.[31] Additionally, some studies focused on one specialized organelle of interest such as the secretory lysosome,[32] the endosomal epidermal growth factor receptor signaling targets,[33] and the zymogen granule in pancreatic acinar cells.[34] The fractionation of the proteome into organelle proteomes appears to be a valid strategy for reducing the sample complexity and obtaining information on the localization of proteins.

To efficiently process the highly complex or rare phosphoproteomic samples, an integrated platform combining protein digestion and reduction of digests' complexity is highly demanded. Here, we developed a microfluidic Proteomic Reactor which provides an integrated platform to efficiently and reliably extract, purify, and concentrate complex proteomic samples into nanoliter volumes.[35] We recently extended the application of the Proteomic Reactor into a multiplex format[36] and for analyzing protein PTMs such as ubiquitin[37] and glycosylation.[38] Here, we report the development of a microfluidic phosphoproteomic reactor that integrates (i) highly efficient protein processing and digestion, and (ii) phosphopeptide enrichment by Ti-IMAC into a single microfluidic platform. We first demonstrate that this integrated approach provides better sensitivity than the conventional phosphopeptide mapping approach. We then show that combining the phosphoproteomic reactor with subcellular fractionations can identify over 1000 nonredundant phosphopeptides from 621 phosphoproteins that are localized in 15 different subcellular fractions from human HUH7 cell lines.

Materials and Methods

Materials and Reagents. Proteins of α-casein, β-casein, bovine serum albumin (BSA), and myoglobin were purchased from Sigma (St. Louis, MO). Modified trypsin came from Promega (Madison, WI). Phosphopeptide standards of VNQLG*p*TLSESIK (P1) and VNQLGTL*p*SE*p*SIK (P2) were obtained from Waters (Milford, MA). The following primary antibodies were commercially ordered from the sources indicated: mouse anti-early endosomal antigen 1 (EEA1; Abcam), rabbit anti-lamp1 (Cell Signaling Technology), rabbit anti-TGN46 (Abcam), rabbit anti-calnexin (Stressgen), goat anti-lamin A/C antibody (Cell Signaling Technology). The secondary antibodies of anti-mouse antibody, anti-rabbit antibody and anti-donkey goat antibody were purchased from Cell Signaling Technology.

Acetonitrile (ACN) with 0.1% formic acid, water with 0.1% formic acid, and orthophosphoric acid (85%, v/v) were purchased from J.T. Baker (Phillipsburg, NJ). Strong cation exchange beads (10 μm) and C18 SepPak cartridges were obtained from Polymer Laboratories, Varian, Inc. and Waters (Milford, MA), respectively. All other chemicals, including ammonium bicarbonate (ABC), triethylammonium bicarbonate (TEAB), dithiothreitol (DTT), iodoacetamide (IAA), trifluoroacetic acid (TFA) and $TiCl_4$ in 0.1 M HCl solutions were supplied by Sigma (St. Louis, MO).

The polymer beads with phosphate groups for phosphopeptide enrichment were made using a modification of the protocol previously reported by Zhou et al.[19] Briefly, Ti-IMAC beads were made by incubating 100 mg of polymer beads in 10 mL of $TiCl_4$ in 0.1 M HCl solution at room temperature overnight. The Ti-IMAC beads were then centrifuged at 20 000*g* for 2 min. The supernatant was removed, and the Ti-IMAC beads were extensively washed with 30% ACN in 0.1% TFA to remove any residual Ti ions. Finally, the Ti-IMAC beads were dispersed into 30% ACN in 0.1% TFA and stored at 4 °C.

Preparation of Standard Protein Digests. The standard phosphoprotein mixture was composed of α-casein and β-casein which were dissolved in 50 mM ABC (pH ∼8) and digested in a 1:40 (m/m) with trypsin overnight at 37 °C. The standard nonphosphoproteins were made by dissolving BSA (6.6 mg) and myoglobin (1.8 mg) in 50 mM ABC (pH ∼8). The solution was then heated at 70 °C for 5 min, and the protein disulfide bonds were reduced with 5 mM DTT at 56 °C for 20 min. Once the protein solutions cooled down to room temperature, the proteins were alkylated using 10 mM IAA in the dark at room temperature for 30 min. The solution was then digested by adding trypsin in a 1:40 ratio (m/m) at 37 °C trypsin overnight. The tryptic peptides were acidified with 10% TFA to obtain a pH of 2−3. The peptides were desalted using a pre-equilibrated C18 column. After washing the column with 0.1% TFA, the peptides were eluted using 80% ACN in 0.1% TFA, lyophilized, and stored at −20 °C.

Phosphoproteomic Reactor. The microfluidic phosphoproteomic reactor was made by integrating the proteomic reactor and the phosphopeptide enrichment reactor (Figure 1). The Proteomic Reactor was built as previously described.[38] Briefly, for the study of standard proteins and phosphoproteins mixtures, 4 cm of a 200 μm i.d. fritted fuse silica tube was packed with strong cation exchange (SCX) beads, while for the study of subcellular fractions, 8 cm of a 700 μm i.d. fritted fuse silica tube was packed with SCX beads. The phosphopeptide enrichment reactor was built by packing 4 cm of Ti-IMAC beads into 200 and 700 μm i.d fritted fuse silica tubes, respectively.

The standard protein mixture 1, which consisted of 200 fmol of α-casein, 200 fmol of β-casein, 20 pmol of BSA, and 20 pmol of myoglobin, was used to test the specificity of the phosphoproteomic reactor. The standard protein mixture 2, which consisted of 2 fmol of α-casein and 2 fmol of β-casein, was used to test the sensitivity of the phosphoproteomic reactor.

As illustrated in Figure 1, prior to the injections of the standard protein mixtures and complex biological samples (cell lysate or subcellular fractions), the samples were mixed with trypsin at a mass ratio of 5:1, acidified to a final concentration of 50 mM H_3PO_4, and introduced into the Proteomic Reactor. At low pH, the protein sample and the trypsin carry multiple positive charges and form strong ionic bonds with the SCX beads present in the Proteomic Reactor, allowing rapid concentration of the proteins without the need for protein precipitation. The Proteomic Reactor also efficiently removes substantial interferents such as DNA, RNA, ATP and others molecules which would otherwise compete with the phosphopeptides for binding on the phosphopeptide enrichment reactor.

The proteins bound to the Proteomic Reactor were then subjected to a series of protein reactions that included disulfide bond reduction by infusing DTT (100 mM DTT in 10 mM ABC)

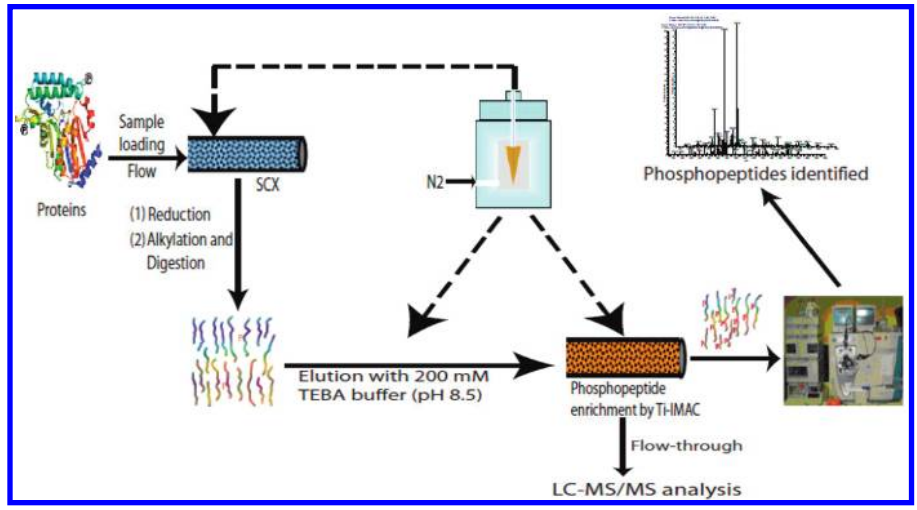

Figure 1. Schematic representation of the phosphoproteomic reactor.

followed by simultaneous alkylation and trypsin digestions by changing the initial buffer to the digestion buffer (100 mM Tris-HCl, 10 mM IAA). After 2 h digestion at room temperature, the peptides generated on the Proteomic Reactor were eluted using 30 μL (for standard protein samples) and 500 μL (for subcellular fractions) of 200 mM TEAB buffer (pH 8.5), and then were concentrated by SpeedVac. The phosphopeptide enrichment reactor was first washed with 10 or 100 μL of 30% ACN in 0.1% TFA. The dried peptide samples were dissolved in 60 μL of 80% ACN in 6% TFA and were continuously flowed through the phosphopeptide enrichment reactor by applying 20 psi of nitrogen pressure. Next, the phosphopeptide enrichment reactor was washed with 30 μL (for standard protein samples) and 300 μL (for subcellular fractions) of 50% ACN in 0.6% TFA containing 200 mM NaCl to remove any nonspecific adsorbed peptides. A second wash of the same volumes of 30% ACN in 0.1% TFA was also performed. The bound phosphopeptides were eluted using 10 μL (for standard protein samples) and 100 μL (for subcellular fractions) of 10% $NH_3.H_2O$. The eluted phosphopeptides were lyophilized prior to LC-MS/MS analysis.

Cell Culture of HUH7 Cells. HUH7 cells were cultured in 15 cm plates with high glucose Dulbecco's modified Eagle's medium at 37 °C in a 5% CO_2 humidified incubator. The Dulbecco's modified Eagle's medium was supplemented with 10% fetal bovine serum, 100 μg/mL penicillin, 100 μg/mL streptomycin, and 50 μg/mL antimycotic.

Subcellular Fractionation of HUH7 Cells and Western Blots. The cell fractionation was performed as depicted in Figure 2a. Briefly, cells at 80% confluency were washed twice with 1 mL of PBS buffer at 4 °C after the growth medium was removed. Next, the cells were detached from the dishes using a cell scraper and pooled into a 15 mL tube for centrifugation (500*g*, 4 °C, 5 min). After removing the supernatant, the cells were resuspended in 3 mL of homogenization buffer (250 mM sucrose, 3 mM imidazole, 1 mM EDTA, pH 7.4) containing protease inhibitors (Complete EDTA-free) and phosphatase inhibitors (Phosphostop) obtained from Roche. The cell suspension was homogenized by 20 stroke passes through a ball bearing homogenizer at 4 °C. Unbroken cells and nuclei were removed by centrifugation (1000*g* at 4 °C, 10 min). The first supernatant was transferred to a 30 mL thick-walled centrifuge tube for further centrifugation at 10 000 rpm for 10 min (4 °C) to remove the nucleus and mitochondria. The second supernatant was collected and labeled as post nuclear supernatant (PNS) for further centrifugation. A total of 200 μL of the PNS was kept for Western blot analysis. As well, the pellet containing the nucleus and mitochondria was also stored at −80 °C. The remaining PNS was transferred on top of a 10 mL 10−40% continuous sucrose gradient containing the homogenization buffer. The sucrose gradient was spun for 4 h at 40 000 rpm andf 800 μL fractions were collected from the top to the bottom of the tube. A 200 μL aliquot of each fraction was used for Western blots.

Six microliters of a 5× SDS sample buffer containing 15% β-mercaptoethanol was added to an aliquot (30 μL) of each fraction and boiled for 5 min. Samples were run on 10% SDS-PAGE and transferred to a nitrocellulose membrane. After they were blocked with 5% milk in TBS-T for 1 h at room temperature, the membranes were exposed overnight at 4 °C to the primary antibodies for proteins markers of organelles (anti-goat lamin for nuclear contamination, anti-mouse EEA1 for late endosomes, anti-rabbit Lamp-1 for lysosomes, anti-rabbit TGN46 for trans-golgi network, and anti-rabbit Calnexin for endoplasmic reticulum). All the primary antibodies were used at a dilution ratio of 1:1000 (v/v) with 5% milk in TBS-T, while the corresponding secondary antibodies were used at a dilution ratio of 1:5000 (v/v) in 5% milk in TBS-T. Finally, chemiluminescence was used for immunoreactivity.

Mass Spectrometry Analysis. The enriched phosphopeptides eluted from the phosphoproteomic reactor were reconstituted with 25 μL of 5% FA and loaded on a 200 μm × 50 mm fritted fused silica precolumn packed in-house with 5 cm of reverse phase Magic C18AQ resins (5 μm; 200-Å pore size; Michrom Bioresources; Auburn, CA) using a 1100 micro-HPLC system (Agilent Technologies, Santa Clara, CA). The separation of phosphopeptides was performed on an analytical column (75 μm i.d. × 50 mm) packed with the same beads. The phosphopeptides were eluted during a 70 min gradient of 5−35% ACN (v/v) containing 0.1% formic acid at an eluent flow rate of 200 nL/min after in-line flow splitting.

The HPLC was interfaced to an ESI LTQ linear ion trap mass spectrometer (Thermo Electron, Waltham, MA) and the LTQ instrument was operated in positive ion mode. A voltage of 1.8 kV was applied to generate the electrospray ionization. The instrument was operated in a data-dependent mode which automatically switched between MS, MS/MS, and MS/MS/MS. A full scan MS was first performed to detect potential peptides which was then followed by five data-dependent MS/MS.

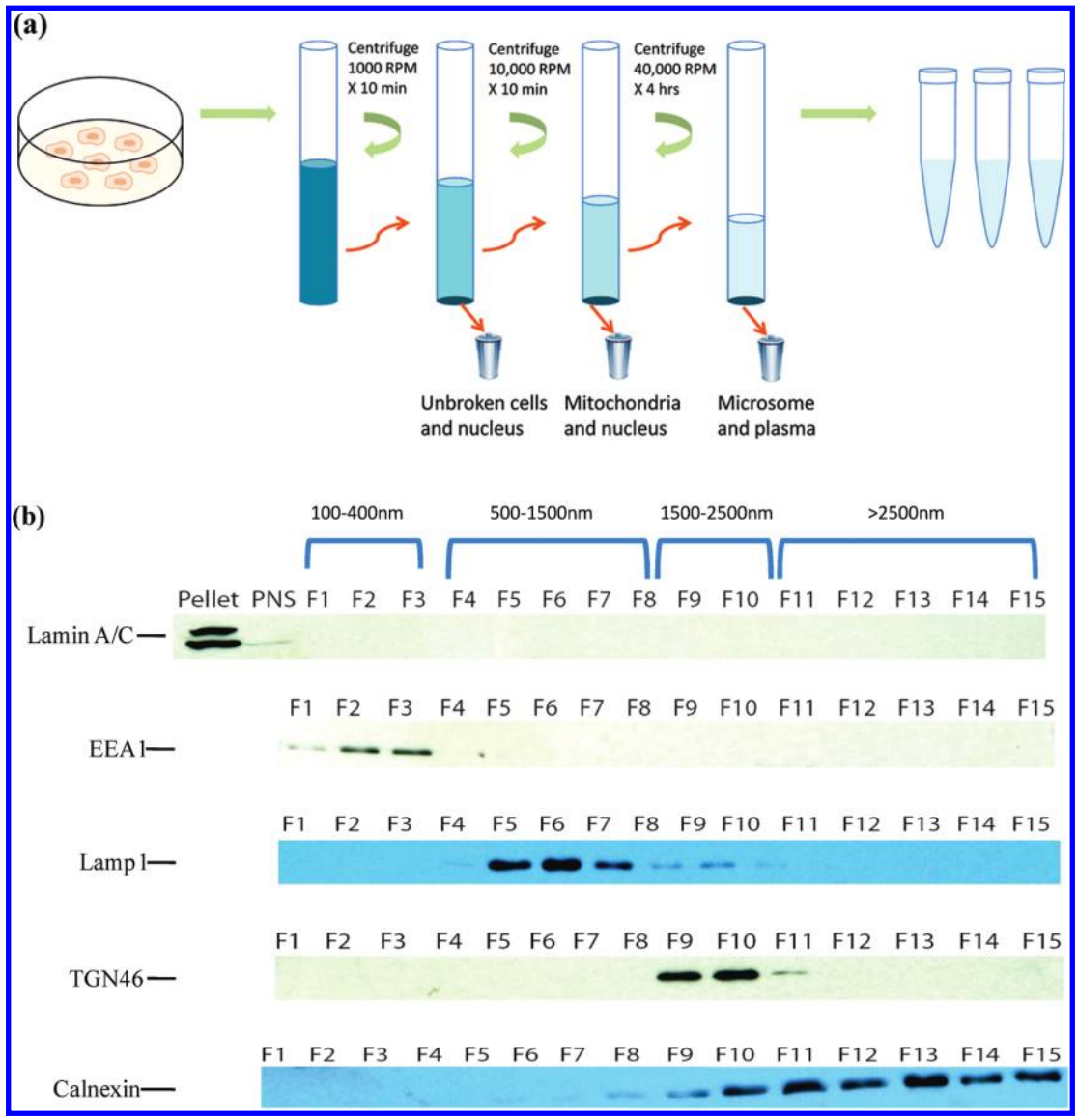

Figure 2. (a) Outline of isolation of organelles by subcellular fractionation of HUH7 cells. *(1), (2),* HUH7 cells were homogenized. *(3)* The homogenate was centrifuged to remove cell pellet and nuclei. *(4)* The supernatant 1 was further centrifuged to remove nuclei and mitochondria. *(5)* The PNS was layered onto a continuous sucrose gradient and organelles were separated. Fifteen fractions were collected starting at the bottom of the tube. (b) Western blots analysis of the fractions for the presence of lamin A/C (Nucleus marker), EEA 1 (early endosome marker), Lamp1 (lysosome marker), TGN46 (trans-golgi network marker), and Calnexin (endoplasmic reticulum marker).

Subsequently, MS/MS/MS were automatically triggered when the 10 most intense peaks from the MS/MS spectrum corresponded to a neutral loss event of 98 m/z, 49 m/z and 32.7 ± 1 Da for the precursor ion with 1+, 2+, 3+ charge states, respectively.

Database Searching and Data Analysis. Peak lists were generated from the raw file using Mascot Distiller 2.0.0.0 (Matrix Science, London, U.K.) to export *mgf files. For each MS/MS, individual peak lists were generated by assuming that the peptide carried a 2+ and a 3+ charge. The MS/MS spectra for the standard protein mixtures were searched against the protein mixture sequence database to which 20 standard protein sequences were added. For the subcellular fractions, MS/MS data were searched against the International Protein Index (version 3.47, 72 079 protein entries; European Bioinformatics Institute, www.ebi.ac.uk/IPI/) using Mascot 2.2.02 (Matrix Science Ltd., London, U.K.). A decoy database search was also performed in a concatenated decoy human database by Mascot. All searches were done using the following criteria: only tryptic peptides with up to two missed cleavage sites were allowed; the mass tolerance was set to 2 Da for MS and 0.8 Da for MS/MS fragment ions; carbamidomethyl was set as a fixed modification; phosphorylation (79.96633 Da) on serine, threonine, and tyrosine, and oxidation (15.99491 Da) on methionine were specified as variable modifications. The false discovery rate of protein identification was limited by accepting only the results with a mascot score >30 ($P < 0.05$). The spectra of all the identified phosphopeptides were manually inspected to ensure that the peak corresponding to the neutral loss of phosphoric acid could be found in the MS/MS/MS spectrum. Data were deemed acceptable if at least 3 successive y- or b-ions were present (or y-++ or b-++ ions if the charge state of the peptide was greater than 2+). The false discovery rate for each fractionation was less than 1%. All the identified

phosphorylation sites were compared to the known sites reported in Swiss-Prot (http://www.expasy.ch/sprot/) and Phosphosite (www.phosphosite.org). Novel phosphorylation sites were additionally annotated.

Network Generation. The proteins in each fraction were first imported as network graphs in Cytoscape version 2.6.2 using the intact Web service client and the Cytoscape spring embedded layout. The proteins found in each fraction were colored in blue in order to better visualize the protein of interest. The union and the intersection of fractions 1−3, 5−7 and 14 to 15 were created using the merge network plugin installed by default in cytoscape (data not show). A Venn diagram from some of the fractions was created using the smartdraw software.

Enrichments. The enrichment pie chart was created using a plugin called ClueGO version 1.1 developed by Bindea et al.[56] ClueGO was used in combination with GOlorize version 2.4.[57] The enrichment test that was based on the hypergeometric distribution was perfomed on each protein fraction. The Bonferroni adjustment was used to correct the *P*-value for the terms and the groups generated by ClueGO. The fusion criteria were used on the related terms that have similar associated genes. A kappa score of 0.3 was used to group the cellular component of the terms. A higher kappa score indicates a higher connectivity between closely related terms with similar associated genes. Also, the calculated kappa score was used to define functional groups.

Results and Discussion

Development of the Phosphoproteomic Reactor. Mass spectrometry based phosphoproteomics is a crucial technique for the study of the phosphoproteome. Researchers have demonstrated the high potential of large-scale mapping of phosphoproteomes.[1,5,39−42] However, many limitations remain in terms of efficient sample processing which often leads to larger amounts of samples required per analysis and the lack of information produced on the subcellular localization of the phosphoproteins.

Here, we present a novel platform, termed the "phosphoproteomic reactor" that efficiently processes, enriches, and analyzes phosphoproteomic samples by mass spectrometry. Briefly, the phosphoproteomic reactor is composed of two modular microfluidic devices (Figure 1). The first module consists of a microfluidic proteomic reactor capable of extracting proteins from complex biological samples, reduces proteins, and simultaneously performs alkylation and enzymatic digestion of proteins. In the second module, the peptides from the first device are lyophilized, reconstituted in a loading buffer, and introduced into a microfluidic Ti-IMAC phosphopeptide enrichment reactor. We selected TEAB as the sample loading buffer because it was previously reported to be compatible with phosphopeptide enrichment by Fe-IMAC.[43] We confirmed that the TEAB buffer is compatible with Ti-IMAC. This change in buffer compared to previous Ti-IMAC protocols eliminates the time-consuming desalting on a C18 reverse phase column. After extensive washes to remove nonspecific adsorption, the bound phosphopeptides are eluted, lyophilized, and analyzed by HPLC-ESI-MS/MS analysis.

Performance of the Phosphoproteomic Reactor Using Standard Protein Mixtures. We tested whether the phosphoproteomic reactor performs better than conventional Ti-IMAC phosphoprotein analyses (see Materials and Methods). Two standard protein mixtures were used to compare the performance. The first mixture consisted of 0.2 pmol of α-casein and

Table 1. List of Phosphorylated Peptides Identified by the Phosphoproteomic Reactor and Conventional Phosphopeptide Enrichment Coupled with LC-MS/MS[a]

			phosphoproteomic reactor		conventional phosphopeptide enrichment	
no.	$[M + H]^+$	phosphorylation sites	200 fmol	2 fmol	200 fmol	2 fmol
α1	1466.61	1	√	√	√	
α2	1481.61	1	√			
α3	1593.84	2	√			
α4	1660.91	1	√	√		√
α5	1862.71	1	√		√	
α6	1927.73	2	√	√	√	
α7	1942.53	2	√	√	√	
α8	1952.06	1	√			
α9	2613.34	2	√			
α10	2716.75	2	√			
α11	2871.22	2	√			
β1	2061.83	1	√	√	√	√
β2	2431.36	1	√			

[a] Overview of the observed phosphopeptides derived from tryptic digests of 200 fmol of α-casein and β-casein in 20 pmol of BSA, and 2 fmol α-casein and β-casein.

β-casein to which 100 times more BSA and mygologbin (20 pmol each) were added. This mixture was used to test the performance of the phosphoproteomic reactor for enriching phosphorylated proteins in the presence of high levels of nonphosphorylated proteins. After the standard protein mixture was processed on the phosphoproteomic reactor, the resulting phosphopeptides were analyzed by LC-MS/MS. A total of 13 phosphopeptides from α-casein and β-casein were identified using the phosphoproteomic reactor, while only 5 phosphopeptides were identified using the conventional approach (Table 1).

The second standard protein mixture consisted of 2 fmol of α-casein and β-casein, and it was used to compare the limit of detection of both approaches. Again, the phosphoproteomic reactor identified 5 phosphopeptides, while the conventional Ti-IMAC approach only identified 2 phosphorylated peptides (Table 1). These results clearly demonstrate that the phosphoproteomic reactor provides significant improvement for phosphopeptide enrichment over the commonly used phosphopeptide enrichment workflow. The phosphoproteomic reactor, therefore, performs efficient enrichment, sample cleanup, and digestion on proteomic Reactor, and reduces sample handling.

We also investigated whether the phosphoproteomic reactor is more efficient at recovering the phosphopeptides than the conventional approach. To test for the phosphopeptide recovery, aliquots of a mixture of 20 pmol of BSA and myoglobin were processed in parallel on the Proteomic Reactor and in-solution. Then, 200 fmol of standard phosphopeptides (VNQLGpTLSESIK and VNQLGTLpSEpSIK) were added to the solutions. The mixtures were analyzed with the phosphoproteomic reactor and the conventional Ti-IMAC method followed by HPLC-ESI-MS/MS. The recovery of the phosphopeptides was evaluated by comparing the peak areas in the extracted ion chromatograms against the peak area of the standard phosphopeptide that was directly injected on the HPLC-MS/MS ($n = 3$, Table 2). The recovery of the enriched phosphopeptides by the phosphoproteomic reactor was nearly 100% and was statistically not different than the recovery from the conventional method. This means that the enhanced perfor-

Table 2. Overview of the Recovery[a] of Standard Phosphopeptides by the Phosphoproteomic Reactor and the Conventional Phosphopeptide Enrichment Method

peptide sequence	phosphorylation sites	charge	phosphoproteomic reactor ± SD ($n = 3$)	conventional phosphopeptide enrichment ± SD ($n = 3$)
VNQLG*p*TLSESIK	1	2	95.4 ± 9.8%	76 ± 15.5%
VNQLGTL*p*SE*p*SIK	2	2	86.7 ± 14.8%	65 ± 18.9%

[a] (The standard phosphopeptides were spiked into the digests on proteomic reactor and underwent the enrichment procedure by phosphoproteomic reactor. Recovery was calculated as the peak area ratio of the standard phosphopeptide by phosphoproteomic reactor or conventional phosphopeptide enrichment and without enrichment).

mance of the phosphoproteomic reactor is due mainly to the better processing of proteins on the reactor device.

Subcellular Organelle Phosphoproteome from HUH7 Cells. The performances of the phosphoproteomic reactor were tested using complex samples obtained from organelle fractions from HUH7 cells. Briefly, the organelles from HUH7 cells were separated on the basis of their size and density by continuous sucrose gradient subcellular fractionation as shown in Figure 2a (see Materials and Methods). We examined the profiles of organelles by Western blots using specific antibodies against "marker proteins" that specifically localized to different organelles including the early endosome (EEA1), lysosome (Lamp-1), trans-golgi network (TGN46), endoplasmic reticulum (calnexin), and the nucleus (lamin A/C) (Figure 2b). The known size range for these organelles is also reported in Figure 2. This does not mean that the fractions are exclusive to a specific organelle. Other organelles exist that fall within these size ranges; however, it is not practical to test for all of them. Furthermore, it is likely that large macromolecules and complexes, such as microtubules, can focus on the sucrose gradient within the low molecular range. Although nuclear contamination was tested using lamin A/C, a marker for the nuclear envelope, it does not preclude the nuclear proteins from subnuclear structures to be present in the fractions. Furthermore, nuclear proteins have been reported to be present in the ER.[45−48] The Western blots for other protein markers suggest enrichment of the endosomes (EEA1) in fractions 1−3, the lysome (Lamp-1) in fractions 5−9, and the trans-golgi network (TGN-46) in fractions 9−11. The presence of ER in fractions 9−15 was corroborated by immunoblotting with specific antibody to calnexin. As expected, an overlap between the fractions for lysosome, golgi, and ER was found in agreement with the literature.[27]

All the 15 fractions that contained organelles were analyzed using the phosphoproteomic reactor followed by HPLC-MS/MS analysis. A total of 1141 unique phosphopeptides from 621 phosphoproteins were identified (see Supplementary Table) based on the MASCOT search engine ($p < 0.05$, false discovery rate lower than 1% for each fraction by decoy database search). Furthermore, 215 novel phosphorylation sites were identified based on comparing our results with the known phosphorylations sites reported in the Phosphosite and Swiss-Prot Databases. The newly identified phosphorylation sites are listed in the Supplementary Table S2. In comparison with recent systematic mapping of thousands of phosphorylation sites,[39,49] we have identified a high percentage of novel phosphorylation sites.

We also analyzed the distributions of the phosphoproteins across the different subcellular fractions. We computed the number of phosphopeptides observed per unique protein across the 15 fractions (see Materials and Methods) for a total of 2550 observed phosphopeptides. As well, 65% of the unique phosphoproteins were seen in more than one fraction. We then performed a clustering analysis of the number of phosphorylated peptides per phosphoproteins in the different fractions. The results clearly indicate that the phosphorylated proteins cluster within specific fractions (Figure 3) and are different than the clustering of random data (figure not shown). For simplicity, we provide three examples of phosphoproteins in different cluster regions. The first phosphoprotein, called WD repeat containing protein 44, was observed in the region that clustered in the 100−400 nm size, which coincides with the markers for the endosome. WD repeat containing protein 44 is a downstream effector of RAB11, it is involved in vesicle recycling, and it localizes to the endosome membrane.[50] The second phosphoprotein of interest, called membrane-associated progesterone receptor component 1, was observed in the size range >2500 nm, which coincides with the marker for the ER.[51] PGRMC1 binds progesterone and has been reported to be mostly located in intracellular membranes. In liver cells, it colocalizes with the endoplasmic reticulum.[52] The third phosphorylated protein, called microfibrillar-associated protein 1, is in a cluster region that is present in all of the fractions. Microfibrillar-associated protein 1 is a secreted protein that is associated with extracellular microfibrils.[53] It is reasonable that secreted proteins would be observed across different secretory organelles.

We have analyzed the known protein interactions for the phosphoproteins observed in three different size ranges of organelles (100−400, 500−1500, and >2500 nm). A subgroup of the phosphoproteins in each size range can be linked through protein interactions (Figure 4). Interestingly, it is very apparent in the network that some phosphoproteins have multiple interactors. For example, the phosphorylated protein CRK, present in Figure 4A (highlighted), is an adaptor protein that has an essential role in many biological processes including the phagocytic and endocytic pathways, cell proliferation, cell adhesion and migration, and others.[54] Its presence in the 100−400 nm organelle region is consistent with its known role in the endocytic pathway. The second example, protein Traf2- and Nck-interacting kinase (TNIK), observed in Figure 4B, also has many known interacting partners. TNIK is a serine/threonine kinase that responds to cellular stress and acts on the JUN N pathway. It is also involved in cytoskeletal regulation and is known to localize to the perinuclear region. Its presence in the 500−1500 nm organelle region is consistent with the known increased concentration of late endosomes and lysosomes at the perinuclear region during interphase. Finally, the third example is the membrane-associated progesterone receptor component 1 (PGRMC1) which was observed as a phosphoprotein in the >2500 nm organelle region (Figure 4C) and coincides with the ER region. PGRMC1 is known to localize to the ER and is involved in the regulation of P450.[55]

We have also tested whether the phosphoproteins observed in the different size ranges of organelles are known to interact. The overlap for direct interactions between the phosphopro-

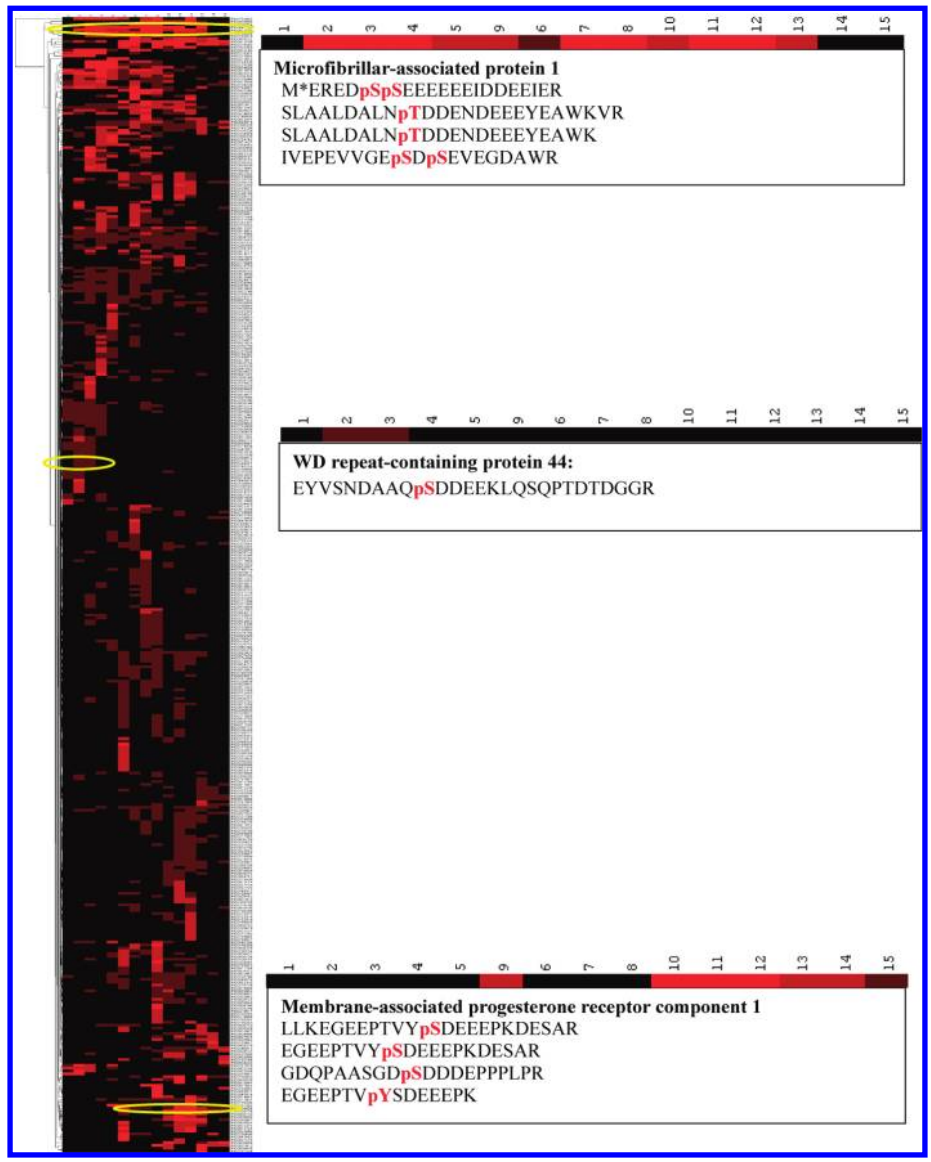

Figure 3. Hierarchical clustering of the phosphoproteins across the subcellular fractions. The number of phosphopeptides identified per proteins across the 15 fractions was used for the hierarchical clustering. Only the phosphoproteins observed in more than one fraction or observed in only one fraction but with two or more unique phosphopeptides were included in the analysis. Three phosphoproteins and the identified phosphopeptides from different regions are provided in insets. The left axis represent the cluster tree while the right axis represents different proteins identified by their IPI number. The top axis is the fraction number and the intensity of the elements represented the number of phosphopeptides observed in a specific fraction. Three insets representing three different phosphoproteins observed in different regions of the cluster are provided for illustration purpose.

teins observed in our experiment and across different fractions is very limited. Only 16 phosphorylated proteins have been shown to directly interact with other phosphoproteins across the three networks representing background phosphoproteins. Furthermore, no other phosphoproteins were observed to directly interact with phosphoproteins between the 100−400 and the 500−1500 organelle regions, which indicate a limited cross-talk in phosphoprotein networks between different regions. Moreover, the analysis of the GO annotation between the phosphorylated proteins found in the different fractions (Figure 5) clearly indicates that different GO localization subcategories are enriched in different size ranges of organelles. As expected, the percentage of phosphoproteins annotated as nuclear increases from the smaller to the larger organelles. Contaminant proteins are expected to be diffused across multiple fractions. Although nuclear phosphoproteins were observed in different fractions, they are not contaminants, as each phosphoprotein was focused in very specific fractions. Instead, the presence of nuclear phosphoproteins is likely due to different subnuclear structures that fall within the different fraction size ranges. As well, phosphoproteins annotated to be present in the endosome, peroxisome, cell surface and secreted were predominantly observed in fractions F1−F3. Finally, phosphoproteins annotated as ER were only observed in fractions F14 to F15 which is also consistent with the fractionation.

We have described a novel technology, termed the phosphoproteomic reactor, which integrates multiple processes for the analysis of phosphoproteomes. We have demonstrated that this technology performs better than conventional phosphoproteomic approaches using standard proteins. Moreover, the combination of the phosphoproteomic reactor with subcellular

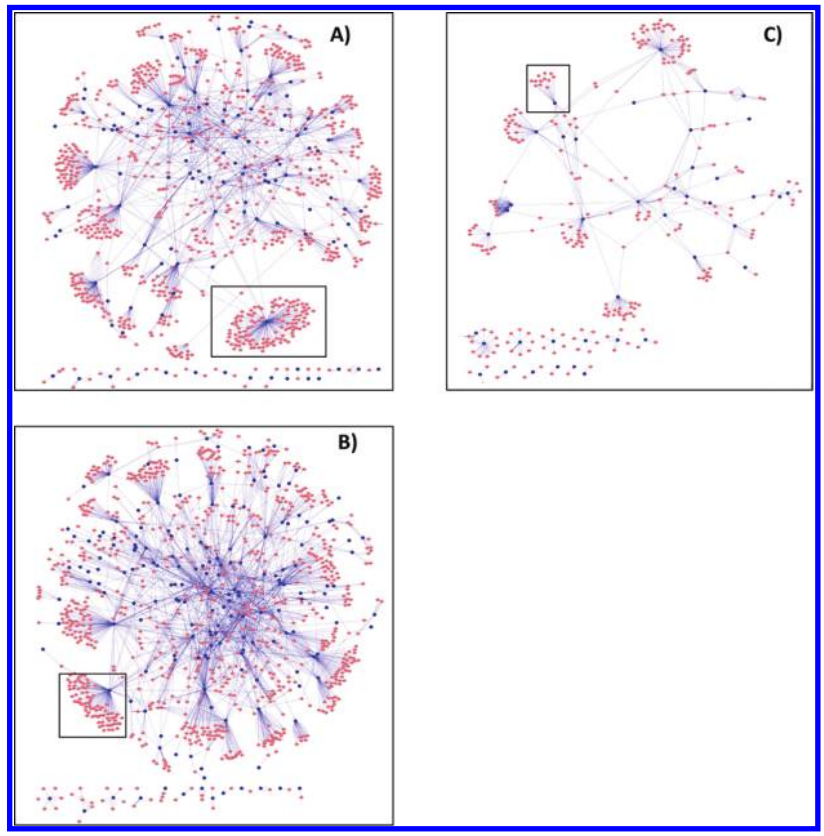

Figure 4. Network of known protein−protein interactions visualized using Cytoscape spring-embedded layout algorithm for three different sizes of organelles: (A) for the 100−400 nm organelle region, (B) for the 500−1500 nm organelle region and (C) for the >2500 nm organelle region. The blue nodes are the phosphoproteins found in the fraction while the orange nodes represent known interactors from the literature (Intact database).

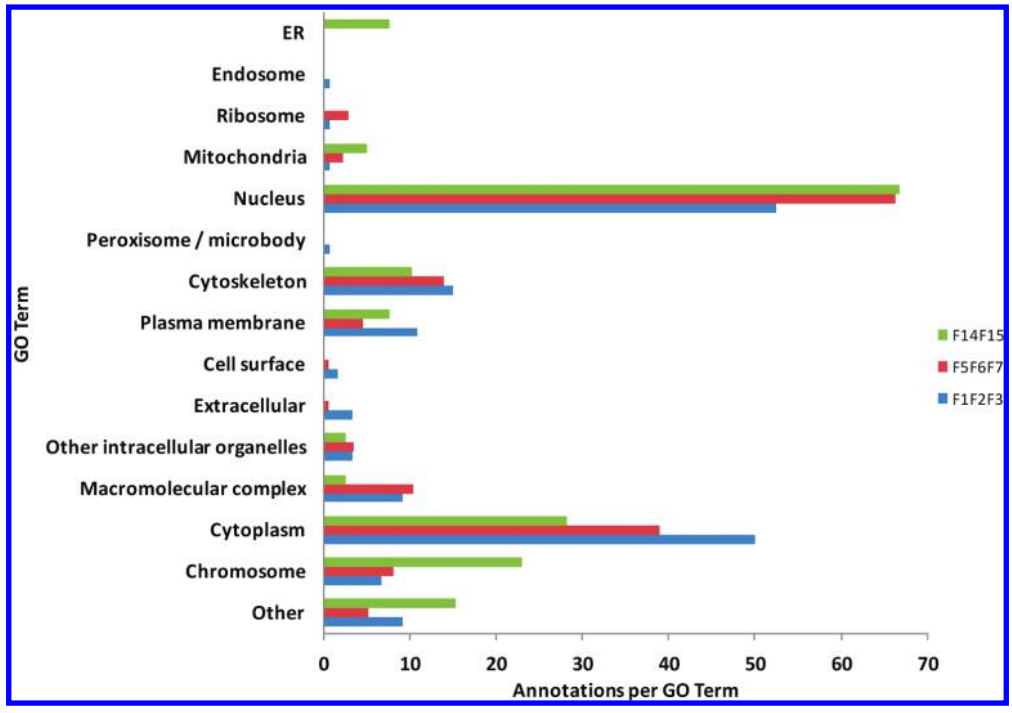

Figure 5. Overview charts of the GO cellular component for the different fraction ranges. The number of proteins per category was normalized to the total number of proteins in each fraction range.

fractionations allowed the identification of phosphorylated proteins based on their subcellular localization.

Abbreviations: LC-MS/MS, liquid chromatography coupled with tandem mass spectrometry; Ti-IMAC, immobilized titanium ion (Ti^{4+}) affinity chromatography; PTM, post-translational modification; HILIC, hydrophilic interaction chromatography; SIMAC, sequential elution from IMAC; CAD, collision-activated dissociation; TEAB, triethylammonium bicarbonate;

ABC, ammonium bicarbonate; DTT, dithiothreitol; IAA, iodoacetamide; ACN,acetonitrile; TFA,trifluoroacetic acid.

Acknowledgment. This project was funded by NSERC, Genome Canada through the Ontario Genomics Institute (2008-OGI-TD-01), and The Province of Ontario. Daniel Figeys acknowledges a Canada Research Chair in Proteomics and Systems Biology. We would like to acknowledge editorial help from Rachel Figeys.

Supporting Information Available: Supplementary Tables 1 and 2 listing the phosphopeptides and phosphorylation sites identified. This material is available free of charge via the Internet at http://pubs.acs.org.

References

(1) Rikova, K.; Guo, A.; Zeng, Q.; Possemato, A.; Yu, J.; Haack, H.; Nardone, J.; Lee, K.; Reeves, C.; Li, Y.; Hu, Y.; Tan, Z.; Stokes, M.; Sullivan, L.; Mitchell, J.; Wetzel, R.; Macneill, J.; Ren, J. M.; Yuan, J.; Bakalarski, C. E.; Villen, J.; Kornhauser, J. M.; Smith, B.; Li, D.; Zhou, X.; Gygi, S. P.; Gu, T. L.; Polakiewicz, R. D.; Rush, J.; Comb, M. J. Global survey of phosphotyrosine signaling identifies oncogenic kinases in lung cancer. *Cell.* **2007**, *131* (6), 1190–203.

(2) Macek, B.; Mann, M.; Olsen, J. V. Global and site-specific quantitative phosphoproteomics: principles and applications. *Annu. Rev. Pharmacol. Toxicol.* **2009**, *49*, 199–221.

(3) Hunter, T. Signaling—2000 and beyond. *Cell* **2000**, *100* (1), 113–27.

(4) Thingholm, T. E.; Jensen, O. N.; Larsen, M. R. Analytical strategies for phosphoproteomics. *Proteomics.* **2009**, *9* (6), 1451–68.

(5) Olsen, J. V.; Blagoev, B.; Gnad, F.; Macek, B.; Kumar, C.; Mortensen, P.; Mann, M. Global, in vivo, and site-specific phosphorylation dynamics in signaling networks. *Cell.* **2006**, *127* (3), 635–48.

(6) Rush, J.; Moritz, A.; Lee, K. A.; Guo, A.; Goss, V. L.; Spek, E. J.; Zhang, H.; Zha, X. M.; Polakiewicz, R. D.; Comb, M. J. Immunoaffinity profiling of tyrosine phosphorylation in cancer cells. *Nat. Biotechnol.* **2005**, *23* (1), 94–101.

(7) Nuhse, T. S.; Stensballe, A.; Jensen, O. N.; Peck, S. C. Large-scale analysis of in vivo phosphorylated membrane proteins by immobilized metal ion affinity chromatography and mass spectrometry. *Mol. Cell. Proteomics* **2003**, *2* (11), 1234–43.

(8) Posewitz, M. C.; Tempst, P. Immobilized gallium(III) affinity chromatography of phosphopeptides. *Anal. Chem.* **1999**, *71* (14), 2883–92.

(9) Larsen, M. R.; Thingholm, T. E.; Jensen, O. N.; Roepstorff, P.; Jorgensen, T. J. Highly selective enrichment of phosphorylated peptides from peptide mixtures using titanium dioxide microcolumns. *Mol. Cell. Proteomics* **2005**, *4* (7), 873–86.

(10) Kweon, H. K.; Hakansson, K. Selective zirconium dioxide-based enrichment of phosphorylated peptides for mass spectrometric analysis. *Anal. Chem.* **2006**, *78* (6), 1743–9.

(11) Nita-Lazar, A.; Saito-Benz, H.; White, F. M. Quantitative phosphoproteomics by mass spectrometry: past, present, and future. *Proteomics* **2008**, *8* (21), 4433–43.

(12) Ficarro, S. B.; McCleland, M. L.; Stukenberg, P. T.; Burke, D. J.; Ross, M. M.; Shabanowitz, J.; Hunt, D. F.; White, F. M. Phosphoproteome analysis by mass spectrometry and its application to Saccharomyces cerevisiae. *Nat. Biotechnol.* **2002**, *20* (3), 301–5.

(13) Thingholm, T. E.; Jorgensen, T. J.; Jensen, O. N.; Larsen, M. R. Highly selective enrichment of phosphorylated peptides using titanium dioxide. *Nat. Protoc.* **2006**, *1* (4), 1929–35.

(14) Sugiyama, N.; Masuda, T.; Shinoda, K.; Nakamura, A.; Tomita, M.; Ishihama, Y. Phosphopeptide enrichment by aliphatic hydroxy acid-modified metal oxide chromatography for nano-LC-MS/MS in proteomics applications. *Mol. Cell. Proteomics* **2007**, *6* (6), 1103–9.

(15) Wu, J.; Shakey, Q.; Liu, W.; Schuller, A.; Follettie, M. T. Global profiling of phosphopeptides by titania affinity enrichment. *J. Proteome Res.* **2007**, *6* (12), 4684–9.

(16) Thingholm, T. E.; Jensen, O. N.; Robinson, P. J.; Larsen, M. R. SIMAC (sequential elution from IMAC), a phosphoproteomics strategy for the rapid separation of monophosphorylated from multiply phosphorylated peptides. *Mol. Cell. Proteomics* **2008**, *7* (4), 661–71.

(17) McNulty, D. E.; Annan, R. S. Hydrophilic interaction chromatography reduces the complexity of the phosphoproteome and improves global phosphopeptide isolation and detection. *Mol. Cell. Proteomics* **2008**, *7* (5), 971–80.

(18) Feng, S.; Ye, M.; Zhou, H.; Jiang, X.; Zou, H.; Gong, B. Immobilized zirconium ion affinity chromatography for specific enrichment of phosphopeptides in phosphoproteome analysis. *Mol. Cell. Proteomics* **2007**, *6* (9), 1656–65.

(19) Zhou, H.; Ye, M.; Dong, J.; Han, G.; Jiang, X.; Wu, R.; Zou, H. Specific phosphopeptide enrichment with immobilized titanium ion affinity chromatography adsorbent for phosphoproteome analysis. *J. Proteome Res.* **2008**, *7* (9), 3957–67.

(20) Zhou, H.; Watts, J. D.; Aebersold, R. A systematic approach to the analysis of protein phosphorylation. *Nat. Biotechnol.* **2001**, *19* (4), 375–8.

(21) Bodenmiller, B.; Mueller, L. N.; Mueller, M.; Domon, B.; Aebersold, R. Reproducible isolation of distinct, overlapping segments of the phosphoproteome. *Nat. Methods* **2007**, *4* (3), 231–7.

(22) Prieto, J. H.; Koncarevic, S.; Park, S. K.; Yates, J.; Becker, K. Large-scale differential proteome analysis in Plasmodium falciparum under drug treatment. *PLoS One* **2008**, *3* (12), e4098.

(23) Taouatas, N.; Altelaar, A. F.; Drugan, M. M.; Helbig, A. O.; Mohammed, S.; Heck, A. J. Strong cation exchange-based fractionation of Lys-N-generated peptides facilitates the targeted analysis of post-translational modifications. *Mol. Cell. Proteomics* **2009**, *8* (1), 190–200.

(24) Lewandrowski, U.; Zahedi, R. P.; Moebius, J.; Walter, U.; Sickmann, A. Enhanced N-glycosylation site analysis of sialoglycopeptides by strong cation exchange prefractionation applied to platelet plasma membranes. *Mol. Cell. Proteomics* **2007**, *6* (11), 1933–41.

(25) Gilchrist, A.; Au, C. E.; Hiding, J.; Bell, A. W.; Fernandez-Rodriguez, J.; Lesimple, S.; Nagaya, H.; Roy, L.; Gosline, S. J.; Hallett, M.; Paiement, J.; Kearney, R. E.; Nilsson, T.; Bergeron, J. J. Quantitative proteomics analysis of the secretory pathway. *Cell* **2006**, *127* (6), 1265–81.

(26) Kislinger, T.; Cox, B.; Kannan, A.; Chung, C.; Hu, P.; Ignatchenko, A.; Scott, M. S.; Gramolini, A. O.; Morris, Q.; Hallett, M. T.; Rossant, J.; Hughes, T. R.; Frey, B.; Emili, A. Global survey of organ and organelle protein expression in mouse: combined proteomic and transcriptomic profiling. *Cell.* **2006**, *125* (1), 173–86.

(27) Foster, L. J.; de Hoog, C. L.; Zhang, Y.; Xie, X.; Mootha, V. K.; Mann, M. A mammalian organelle map by protein correlation profiling. *Cell* **2006**, *125* (1), 187–99.

(28) Dunkley, T. P.; Watson, R.; Griffin, J. L.; Dupree, P.; Lilley, K. S. Localization of organelle proteins by isotope tagging (LOPIT). *Mol. Cell. Proteomics* **2004**, *3* (11), 1128–34.

(29) Dunkley, T. P.; Hester, S.; Shadforth, I. P.; Runions, J.; Weimar, T.; Hanton, S. L.; Griffin, J. L.; Bessant, C.; Brandizzi, F.; Hawes, C.; Watson, R. B.; Dupree, P.; Lilley, K. S. Mapping the Arabidopsis organelle proteome. *Proc. Natl. Acad. Sci. U.S.A.* **2006**, *103* (17), 6518–23.

(30) Jiang, X. S.; Dai, J.; Sheng, Q. H.; Zhang, L.; Xia, Q. C.; Wu, J. R.; Zeng, R. A comparative proteomic strategy for subcellular proteome research: ICAT approach coupled with bioinformatics prediction to ascertain rat liver mitochondrial proteins and indication of mitochondrial localization for catalase. *Mol. Cell. Proteomics* **2005**, *4* (1), 12–34.

(31) Hall, S. L.; Hester, S.; Griffin, J. L.; Lilley, K. S.; Jackson, A. P. The organelle proteome of the DT40 Lymphocyte cell line. *Mol. Cell. Proteomics* **2009**, *8* (6), 1295–305.

(32) Casey, T. M.; Meade, J. L.; Hewitt, E. W. Organelle proteomics: identification of the exocytic machinery associated with the natural killer cell secretory lysosome. *Mol. Cell. Proteomics* **2007**, *6* (5), 767–80.

(33) Stasyk, T.; Schiefermeier, N.; Skvortsov, S.; Zwierzina, H.; Peranen, J.; Bonn, G. K.; Huber, L. A. Identification of endosomal epidermal growth factor receptor signaling targets by functional organelle proteomics. *Mol. Cell. Proteomics* **2007**, *6* (5), 908–22.

(34) Chen, X.; Walker, A. K.; Strahler, J. R.; Simon, E. S.; Tomanicek-Volk, S. L.; Nelson, B. B.; Hurley, M. C.; Ernst, S. A.; Williams, J. A.; Andrews, P. C. Organellar proteomics: analysis of pancreatic zymogen granule membranes. *Mol. Cell. Proteomics* **2006**, *5* (2), 306–12.

(35) Ethier, M.; Hou, W.; Duewel, H. S.; Figeys, D. The proteomic reactor: a microfluidic device for processing minute amounts of protein prior to mass spectrometry analysis. *J. Proteome Res.* **2006**, *5* (10), 2754–9.

(36) Hou, W.; Ethier, M.; Smith, J. C.; Sheng, Y.; Figeys, D. Multiplexed proteomic reactor for the processing of proteomic samples. *Anal. Chem.* **2007**, *79* (1), 39–44.

(37) Vasilescu, J.; Zweitzig, D. R.; Denis, N. J.; Smith, J. C.; Ethier, M.; Haines, D. S.; Figeys, D. The proteomic reactor facilitates the analysis of affinity-purified proteins by mass spectrometry: application for identifying ubiquitinated proteins in human cells. *J. Proteome Res.* **2007**, *6* (1), 298–305.

(38) Zhou, H.; Hou, W.; Denis, N. J.; Vasilescu, J.; Zou, H.; Figeys, D. Glycoproteomic reactor for human plasma. *J. Proteome Res.* **2009**, *8* (2), 556–66.
(39) Dephoure, N.; Zhou, C.; Villen, J.; Beausoleil, S. A.; Bakalarski, C. E.; Elledge, S. J.; Gygi, S. P. A quantitative atlas of mitotic phosphorylation. *Proc. Natl. Acad. Sci. U.S.A.* **2008**, *105* (31), 10762–7.
(40) Albuquerque, C. P.; Smolka, M. B.; Payne, S. H.; Bafna, V.; Eng, J.; Zhou, H. A multidimensional chromatography technology for in-depth phosphoproteome analysis. *Mol. Cell. Proteomics* **2008**, *7* (7), 1389–96.
(41) Gauci, S.; Helbig, A. O.; Slijper, M.; Krijgsveld, J.; Heck, A. J.; Mohammed, S. Lys-N and trypsin cover complementary parts of the phosphoproteome in a refined SCX-based approach. *Anal. Chem.* **2009**, *81* (11), 4493–4501.
(42) Swaney, D. L.; Wenger, C. D.; Thomson, J. A.; Coon, J. J. Human embryonic stem cell phosphoproteome revealed by electron transfer dissociation tandem mass spectrometry. *Proc. Natl. Acad. Sci. U.S.A.* **2009**, *106* (4), 995–1000.
(43) Tsai, C. F.; Wang, Y. T.; Chen, Y. R.; Lai, C. Y.; Lin, P. Y.; Pan, K. T.; Chen, J. Y.; Khoo, K. H.; Chen, Y. J. Immobilized metal affinity chromatography revisited: pH/acid control toward high selectivity in phosphoproteomics. *J. Proteome Res.* **2008**, *7* (9), 4058–69.
(44) Ficarro, S. B.; Parikh, J. R.; Blank, N. C.; Marto, J. A. Niobium(V) oxide (Nb2O5): application to phosphoproteomics. *Anal. Chem.* **2008**, *80* (12), 4606–13.
(45) Maissel, A.; Marom, M.; Shtutman, M.; Shahaf, G.; Livneh, E. PKCeta is localized in the Golgi, ER and nuclear envelope and translocates to the nuclear envelope upon PMA activation and serum-starvation: C1b domain and the pseudosubstrate containing fragment target PKCeta to the Golgi and the nuclear envelope. *Cell. Signalling* **2006**, *18* (8), 1127–39.
(46) Dawson, T. R.; Lazarus, M. D.; Hetzer, M. W.; Wente, S. R. ER membrane-bending proteins are necessary for de novo nuclear pore formation. *J. Cell Biol.* **2009**, *184* (5), 659–75.
(47) Alves, S. E.; Lopez, V.; McEwen, B. S.; Weiland, N. G. Differential colocalization of estrogen receptor beta (ERbeta) with oxytocin and vasopressin in the paraventricular and supraoptic nuclei of the female rat brain: an immunocytochemical study. *Proc. Natl Acad. Sci. U.S.A.* **1998**, *95* (6), 3281–6.
(48) Fehrenbacher, K. L.; Davis, D.; Wu, M.; Boldogh, I.; Pon, L. A. Endoplasmic reticulum dynamics, inheritance, and cytoskeletal interactions in budding yeast. *Mol. Biol. Cell* **2002**, *13* (3), 854–65.
(49) Swaney, D. L.; Wenger, C. D.; Thomson, J. A.; Coon, J. J. Human embryonic stem cell phosphoproteome revealed by electron transfer dissociation tandem mass spectrometry. *Proc. Natl. Acad. Sci. U.S.A.* **2009**, *106* (4), 995–1000.
(50) Zeng, J.; Ren, M.; Gravotta, D.; De Lemos-Chiarandini, C.; Lui, M.; Erdjument-Bromage, H.; Tempst, P.; Xu, G.; Shen, T. H.; Morimoto, T.; Adesnik, M.; Sabatini, D. D. Identification of a putative effector protein for rab11 that participates in transferrin recycling. *Proc. Natl. Acad. Sci. U.S.A.* **1999**, *96* (6), 2840–5.
(51) Losel, R. M.; Besong, D.; Peluso, J. J.; Wehling, M. Progesterone receptor membrane component 1--many tasks for a versatile protein. *Steroids* **2008**, *73* (9−10), 929–34.
(52) Falkenstein, E.; Schmieding, K.; Lange, A.; Meyer, C.; Gerdes, D.; Welsch, U.; Wehling, M. Localization of a putative progesterone membrane binding protein in porcine hepatocytes. *Cell. Mol. Biol.* **1998**, *44* (4), 571–8.
(53) Fortini, M. E. Notch signaling: the core pathway and its posttranslational regulation. *Dev. Cell* **2009**, *16* (5), 633–47.
(54) Birge, R. B.; Kalodimos, C.; Inagaki, F.; Tanaka, S. Crk and CrkL adaptor proteins: networks for physiological and pathological signaling. *Cell Commun. Signaling* **2009**, *7*, 13.
(55) Hughes, A. L.; Powell, D. W.; Bard, M.; Eckstein, J.; Barbuch, R.; Link, A. J.; Espenshade, P. J. Dap1/PGRMC1 binds and regulates cytochrome P450 enzymes. *Cell Metab.* **2007**, *5* (2), 143–9.
(56) Bindea, G.; Mlecnik, B.; Hackl, H.; Charoentong, P.; Tosolini, M.; Kirilovsky, A.; Fridman, W. H.; Pages, F.; Trajanoski, Z.; Galon, J. ClueGO: a Cytoscape plug-in to decipher functionally grouped gene ontology and pathway annotation networks. *Bioinformatics* **2009**, *25* (8), 1091–3.
(57) Garcia, O.; Saveanu, C.; Cline, M.; Fromont-Racine, M.; Jacquier, A.; Schwikowski, B.; Aittokallio, T. GOlorize: a Cytoscape plug-in for network visualization with Gene Ontology-based layout and coloring. *Bioinformatics* **2007**, *23* (3), 394–6.

PR900767J